ELSEVIER

Theoretical and Applied Fracture Mechanics 24 (1996) 189–196

theoretical and applied fracture mechanics

A stochastic jump and deterministic dynamics model of impact failure evolution with rate effect

M.F. Xia [b], Y.L. Bai [a,*], F.J. Ke [c]

[a] *Laboratory for Nonlinear Mechanics of Continuous Media, Institute of Mechanics, Academia Sinica, Beijing 100080, China*

[b] *Department of Physics, Center for Nonlinear Science, Peking University, Beijing 100871, China*

[c] *Department of Applied Physics, Center of Nonlinear Science, Beijing University of Aeronautics and Astronautics, Beijing 100083, China*

Abstract

Motivated by the observation of the rate effect on material failure, a model of nonlinear and nonlocal evolution is developed, that includes both stochastic and dynamic effects. In phase space a transitional region prevails, which distinguishes the failure behavior from a globally stable one to that of catastrophic. Several probability functions are found to characterize the distinctive features of evolution due to different degrees of nucleation, growth and coalescence rates. The results may provide a better understanding of material failure.

1. Introduction

Failure of solids under external loads has been extensively studied for a long time [1]. Generally speaking, material failure is a non-equilibrium and nonlinear process that involves nucleation, growth and coalescence of microdamages at different rates. The phenomenon depends on the coupling of these effects in addition to their individual rates of energy transfer. Their occurrence may be stochastic or deterministic depending on the ways with which damages are developed.

In recent years, several models have been advanced to explain the behavior of material failure [2–12]. While the results have provided some new insights into the interplay between disorder and failure, they have not delved into the details of rate effects. Based on experimental observations and two-dimensional simulation [14–17], a one-dimensional chain model [15–18] has been developed to study the statistical behavior and rate effect of failure. This model is similar to the 1-D chain of bundles [13]; it can be related to the work on fiber-reinforced composites [19] and has yielded effective results [20].

This paper focuses on two rate processes, i.e. stochastic jump and deterministic dynamics. The model includes nonlinear and nonlocal interaction as well as rate effects and reveals important behavior of failure that differs from the prediction made by models involving percolation, cellular automaton and self-organized criticality (SOC).

2. Model description

A description of failure could involve nucleation, growth, coalescence and healing of microdamages. These processes are rate dependent and could be statistical in character. Assume that an individual

* Corresponding author. Tel. +86 10 256 1284, fax +86 10 254 8133, e-mail balyl@lnm.mech.ac.cn.

SSDI 0167-8442(95)00042-9

microdamage can be characterized by a length scale c. Evolution of the microdamage system can thus be described by the number density of microdamage $n(c,t)$, where t is time. The damage rate follows as

$$R = \lim_{\Delta t \to 0} \left(\frac{1}{\Delta t}\right) \int [n(c, t+\Delta t) - n(c,t)]\, c\, \mathrm{d}c\,. \quad (1)$$

If the damage evolution consists of only one elementary process, then Eq. (1) represents the corresponding damage rate. A physical system may involve four different damage rates R_N, R_G, R_C and R_H corresponding to nucleation, growth, coalescence and healing, respectively. Without denoting their explicit dependence on stress and material parameters, a brief description will be given.

2.1. Nucleation

If n_N denote the nucleation rate, the damage rate R_N due to nucleation may be given by

$$R_N = N_N \bar{c}_N\,, \quad (2)$$

in which N_N stands for

$$N_N = \int n_N(c)\, \mathrm{d}c \quad (3)$$

and $\bar{c}_N$ for

$$\bar{c}_N = \frac{1}{N_N} \int n_N(c)\, c\, \mathrm{d}c\,. \quad (4)$$

2.2. Growth

The rate R_G denotes damage rate due to growth; it takes the form

$$R_G = N_t \bar{A} \quad (5)$$

such that

$$\bar{A} = \frac{1}{N_t} \int A(c)\, n(c)\, \mathrm{d}c\,, \quad (6)$$

with A being the growth rate and N_t the total number, i.e.,

$$N_t = \int n(c,t)\, \mathrm{d}c\,. \quad (7)$$

2.3. Coalescence

Assume that the coalescence can take place between ajacent microdamages only. Denoting the distance between two adjacent microdamages by s, a distribution function by $m(s,u,t)$. $m(s,u,t)\, \mathrm{d}s\, \mathrm{d}u$ may be defined to represent the number of ligaments between adjacent microdamages in the range of $s \sim s + \mathrm{d}s$ and coalescence parameter u in the range of $u \sim u + \mathrm{d}u$. The definition of coalescence parameter u will be given subsequently. Then, the rate of coalescence can be represented by

$$R_c = M \bar{A}_c\,. \quad (8)$$

In Eq. (8)

$$M = \int_0^1 \mathrm{d}u \int m(s,u,t)\, \mathrm{d}s \quad (9)$$

and

$$\bar{A}_c = \frac{1}{M} \int_0^1 \mathrm{d}u \int m(s,u,t) A_c(s,u)\, \mathrm{d}s\,, \quad (10)$$

where m is the distribution of ligaments and $A_C(s,u)$ is the effective coalescence rate of an individual coalescence process, and the condition of coalescence is assumed to be $0 \le u \le 1$.

2.4. Healing

Let h denote the healing probability in unit time. The healing rate is given by

$$R_H = \int h(c)\, n c\, \mathrm{d}c\,. \quad (11)$$

2.5. Experimental observation

Evolution of microdamages [14–17] has been observed experimentally on specimens subjected to planar impact. Two main conclusions are:

– There appears no indication of healing. Also, the growth could be neglected in comparison with nucleation in sub-microsecond load durations. For example in the cases of stress $\sigma \sim (1$ to $7)$ GPa and $t \sim 10^{-7}$ s, there results $N_t \sim 10^8$ m^{-2}, $\bar{A} < 10$ ms^{-1}, $N_N \sim 10^{15}$ m^{-2}s^{-1} and $\bar{c}_N \sim 4 \times 10^{-6}$ m. According to Eqs. (2)

and (5), R_N is greater than R_G by about one order of magnitude. Up to now, there are still no measured data of coalescence rate available. However, it is obvious that coalescence dominates the damaged state, when the system approaches failure.

– Nucleation appears to be a stochastic process while coalescence seems to behave in a deterministic dynamic manner.

3. Stochastic and dynamic behavior

Both stochastic and dynamic behaviors are thus invoked in the model. Several prototypes could prevail depending on the dimensionless ratio R_N/R_C:

Case 1: Pattern dynamics ($R_N/R_C \ll 1$). Nucleation can be neglected. The system is merely controlled by the dynamics of coalescence.

Case 2: Slow jump ($R_N/R_C < 1$). The rate of nucleation is lower than that of coalescence such that nucleation can not be neglected.

Case 3: Fast jump ($R_N/R_C > 1$). The rate of nucleation is higher than that of coalescence, but coalescence still plays an important role.

Case 4: Percolation ($R_N/R_C \gg 1$). Nucleation is dominant, and coalescence can be neglected. The system can thus be treated by the percolation theory.

In general, the evolution related to the coupling of stochastic and dynamic processes could be quite complex. As a first step, consider the simplest system, i.e. a one-dimensional chain [18].

3.1. Pattern dynamics

The one-dimensional chain model consists of N sites. An intact site is denoted by $x_i = 0$, and a broken site by $x_i = 1$. A state, or pattern, of the system is expressed in $X = \{x_i, i = 1, 2, \cdots, N\}$. So the broken number and damage fraction of a state are

$$n = \sum_{i=1}^{N} x_i \tag{12}$$

and

$$p = n/N \tag{13}$$

respectively. The pattern with $p = 0$ is a solid whilst $p = 1$ represents completely failure, denoted by $X_F = \{x_i = 1, i = 1, 2, \cdots, N\}$.

The phase space of the system consists of $\Omega = 2^N$ states, which can be divided into $(N + 1)$ groups according to damage fraction p or n ($n = 0, 1, 2, \cdots, N$), i.e. the macroscopic measure of damage. The total number of the states in group n is

$$\Omega_n = N!/n!(N - n)! \tag{14}$$

Obviously, $\Omega_0 = \Omega_N = 1$.

Now, assume that the evolution of a pattern follows a deterministic and irreversible dynamics. This corresponds to the case of $R_N/R_C \ll 1$ and no healing. In this case, all states in phase space can be divided into two classes: transient and fixed states. The latter states are the final of the pattern dynamics. The pattern dynamics can be described by its flow and the structure of phase space. Each stream line is attracted to one of the fixed states, whereas all the fixed states and their basins of attraction structure the phase space.

In general, the final states of evolutions starting from different states in a given group n may belong to different damage groups. Let $y_{nn'}$ be the number of evolutions starting from group n and ending in group n'. This leads to an $(N + 1) \times (N + 1)$ evolution matrix $Y = \{y_{nn'}\}$. It provides the fundamental statistical information about the evolutions and the structure of phase space. Due to the irreversibility, $y_{nn'} = 0$ if $n > n'$. Diagonal element y_{nn} is the number of fixed states in group n. The element y_{nN} represents the number of states in group n belonging to the basin of failure state X_F. The total number of states in the basin of failure state X_F is

$$M_F = \sum_{n=0}^{N} y_{nN}. \tag{15}$$

Hence, two functions to depict the failure probability can be defined:

$$\Phi(p) = \Phi_n = y_{nN}/\Omega_n \tag{16}$$

and

$$\xi(p) = \xi_n = y_{nN}/M_F. \tag{17}$$

They describe the distribution of the basin of X_F in phase space.

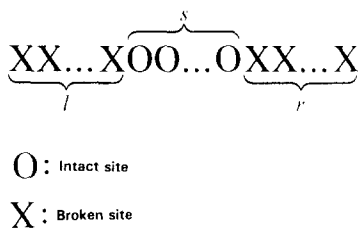

Fig. 1. Sketch of coalescence rule. ○ – intact site, × – broken site.

Divide flows in phase space into two evolution modes according to their final states, i.e., globally stable (GS) and evolution induced catastrophic (EIC). The EIC mode involves evolutions starting from states inside the basin of X_F and ending at a complete failure state, whereas the GS mode includes all the rest, which do not go to failure and keep globally stable. Classification of states in phase space as GS and EIC states can also be made according to their evolution modes.

Based on mechanical analysis and experimental observation, a simple dynamical rule, i.e. the load-sharing rule, has been introduced in composite mechanics [19] and in a 1-D chain of bundles model [13]. Following the rule in [18] such that a s-intact cluster would evolve to break if it separates an r- and an l- broken cluster (see Fig. 1) and satisfies

$$2s/(r+l) \le L_c\,, \tag{18}$$

where L_c is a parameter. If the s-intact cluster is at one end of the chain, take r or l to be zero, respectively. From Eq. (18), the coalescence parameter u in Eqs. (9) and (10) can be written as

$$u = 2s/(r+l)L_c\,. \tag{19}$$

The rule represents a deterministic, irreversible, nonlinear and nonlocal dynamics, especially an automatically enlarging interaction of microdamage without any characteristic length scale. Accordingly, coalescence of broken clusters can occur in all scales and a limitless cascade of coalescence from a small to a large scale may appear. This is the key underlying mechanism of catastrophe induced by the evolution.

From Eq. (18), there prevails a region in phase space known as the transitional region, $p_L < p < p_U$, where GS and EIC states coexist, i.e. $0 < \Phi(p) < 1$. In the limit as $N \to \infty$, it follows that

$$\lim_{N\to\infty} p_L = 0 \tag{20}$$

Table 1
Evolution matrix and Ω_n, $N = 10$ and $L_c = 1.0$

n	n'											Ω_n
	0	1	2	3	4	5	6	7	8	9	10	
0	1	0	0	0	0	0	0	0	0	0	0	1
1	0	10	0	0	0	0	0	0	0	0	0	10
2	0	0	35	8	2	0	0	0	0	0	0	45
3	0	0	0	58	30	12	12	0	0	0	8	120
4	0	0	0	0	47	40	32	0	0	0	91	210
5	0	0	0	0	0	20	28	0	0	0	204	252
6	0	0	0	0	0	0	7	0	0	0	203	210
7	0	0	0	0	0	0	0	0	0	0	120	120
8	0	0	0	0	0	0	0	0	0	0	45	45
9	0	0	0	0	0	0	0	0	0	0	10	10
10	0	0	0	0	0	0	0	0	0	0	1	1

and

$$\lim_{N\to\infty} p_U = 1/(1+\frac{1}{2}L_c)\,. \tag{21}$$

As an example, consider the case of $N = 10$ and $L_c = 1.0$. The total number of states in phase space , which belong to 11 damage groups, is $\Omega = 1024$. The evolution matrix is shown in Table 1. The number of states in the basin of X_F is $M_F = 682$. The lower and upper limit of the transitional region are $p_L = 0.2$ and $p_U = 0.7$, respectively. In the transitional region, the number of states belonging to the failure basin of X_F is $M'_F = 506$. Hence, $M'_F/M_F = 0.7419$. This means that the transitional region plays an impotant role in EIC. The values of Φ_n and ξ_n are shown in Table 2, and $\Phi = \Phi(p)$ is also shown in Fig. 2. Table 3 gives the parameters of transitional regions in several other cases. One can see that the existence and importance of transitional reigon is a common property of the evolution model.

The pattern dynamics can be illustrated with another language. For an r-broken cluster, assume that there are two influence regions with size $\frac{1}{2}rL_c$ attached to its two ends. Then, coalescence may occur provided influence regions of two adjacent broken clusters contact or overlap each other. If so, the $(1+L_c)r$-cluster is an equivalent broken cluster. In this sence, the occurrence of EIC can be related to a percolation of equivalent broken clusters. The equivalent damage fraction is defined as

$$p' = (1+L_c)p\,. \tag{22}$$

Table 2
Probability distribution functions Φ_n and ξ_n, $N = 10$ and $L_c = 1.0$

n	0	1	2	3	4	5	6	7	8	9	10
Φ_n	0	0	0	0.0667	0.4333	0.8095	0.9667	1	1	1	1
ξ_n	0	0	0	0.0117	0.1334	0.2991	0.2977	0.1760	0.0660	0.0147	0.0015

Table 3
Parameters of transitional region

N	5	6	7	8	9	10	10	10
L_c	1	1	1	1	1	1	0.5	2
p_L	0.2	0.1667	0.2857	0.25	0.2222	0.2	0.4	0.1
p_U	0.8	0.6667	0.7143	0.75	0.6667	0.7	0.8	0.5
M_F^L/M_F	0.5385	0.4211	0.5972	0.7376	0.6210	0.7419	0.7637	0.3291

The threshold of percolation is $p' = 1$. Then, the corresponding threshold of the real critical damage fraction is

$$p_c = 1/(1 + L_c)\,. \tag{23}$$

For $L_c = 1.0$, Eq. (23) gives $p_c = 0.5$. Its comparison to the transitional region in the concerned pattern dynamics is shown in Fig. 2. The representation of critical failure due to percolation theory (Case 4) $p_c = 1$ is also shown in Fig. 2. The simulation shows that the boundary between GS and EIC spreads over a wide

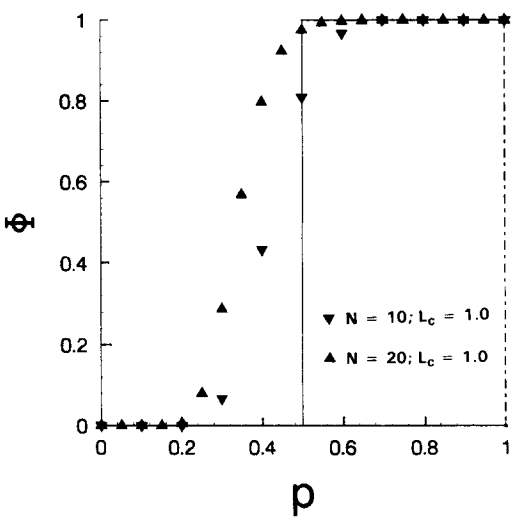

Fig. 2. Failure probability of pattern dynamics, its comparison to equivalent percolation (———) and percolation (Case 4) (— · — · —), and the effect of chain size. ▼: $N = 10$, $L_c = 1.0$; ▲: $N = 20$, $L_c = 1.0$.

transitional region. The differences between the concerned pattern dynamics and percolation can be clarified as follows:

- In the pattern dynamics, the damage fraction p is a state variable and can vary progressively.
- The pattern dynamics cannot be determined by damage fraction itself. It is sensitively dependent on the initial configuration of damage; that is to say, it is pattern-specific.

In addition, the effect of chain size on the pattern dynamics (see Fig. 2) has been examined. Moreover, the thermodynamical limits in Eqs. (20) and (21), $p_L = 0$ and $p_U = 2/3$ when $L_c = 1.0$, provide the two bounds for the transitional region. The results indicate that the characteristics of failure probability Φ is rarely affected by the sizes of the chain. This behavior at pattern dynamics resembles material failure in nature that may be attributed to a certain complex evolution induced catastrophe (EIC). The occurrence of failure should thus be described by a probability distribution function. Especially, the noticeable sample-specific phenomenon in material failure probably corresponds to the pattern-specific behavior of the pattern dynamics.

3.2. *Stochastic jump*

Consider how stochastic jump could affect the damage evolution governed by the above-mentioned pattern dynamics. In fact, the stochastic jump can make a pattern jump from one trajectory to another, from one basin to another, and especially from GS to EIC

mode. Concerning material failure, the jump could induce mode conversion from GS to EIC that play an essential role in the damage evolution. Such a conversion can never happen in the chain system governed by the pattern dynamics discussed in the last section.

A simple selection rule of pattern jump can be introduced as follows:

$$\Delta n = +1 . \tag{24}$$

This implies that the irreversibility, i.e. a jump from a broken site to an intact site is impermissible and in each jump the increment of broken sites is limited by a unit. There are several types of stochastic jumps: from GS to GS, from GS to EIC, and from EIC to EIC. Obviously, the jump from EIC to GS is impossible. Let ν_n be the number of possible jumps from the states in group $(n-1)$ to the states in group n, and let μ_n be the number of jumps from GS to EIC among ν_n jumps. Then, another two probability distribution functions of failure can be defined as

$$\Psi(p) = \Psi_n = \mu_n/\nu_n \tag{25}$$

and

$$\eta(p) = \eta_n = \mu_n/\mu , \tag{26}$$

where

$$\mu = \sum_{n=1}^{N} \mu_n . \tag{27}$$

The functions $\Psi(p)$ and $\eta(p)$ describe the probability of mode conversion from GS to EIC.

Clearly, there are two cases corresponding to slow jump and fast jump discussed earlier.

Slow jump (Case 2). Slow jump refers to the case where the rate of stochastic jump is lower than that of the pattern dynamics. In this case, the mode conversion from GS to EIC is dominated by the jumps from GS fixed states to EIC states, and the jumps from GS transient states are negligible (see Fig. 3a). The number of fixed states in group $(n-1)$ is $y_{n-1,n-1}$ and a state in group $(n-1)$ has $(N-n+1)$ ways of jump:

$$\nu_n = (N-n+1)y_{n-1,n-1} , \tag{28}$$

which involves the jumps from GS to EIC (μ_n) and from GS to GS ($\nu_n - \mu_n$).

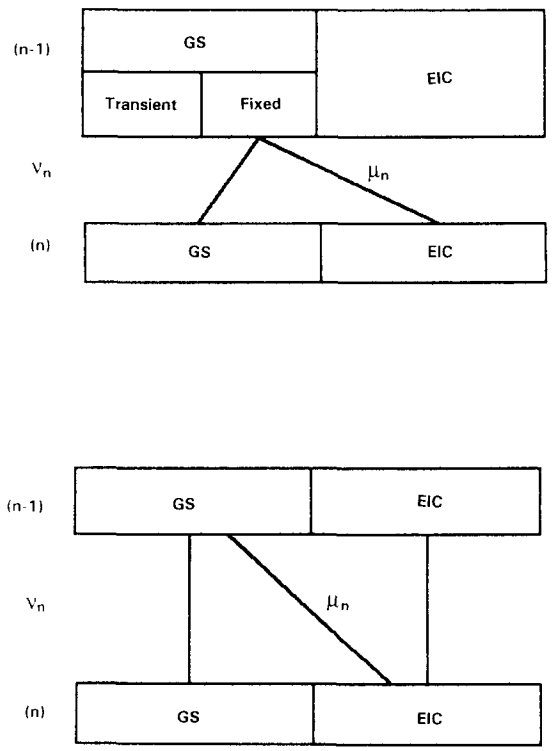

Fig. 3. Schematic of stochastic jumps. (a) Slow jump; (b) Fast jump.

Table 4, gives the results for the case of $N = 10$ and $L_c = 1.0$. The function $\Psi(p)$ and $\eta(p)$ have non-zero values in the region $p_L < p \leq p_U$. $\Psi(p)$ is a monotonical function from 0 at $p = p_L$ to 1 at $p = p_U$ and then cutoff (also see Fig. 4). $\eta(p)$ is a unimodal function and its peak is at $p = p_M = 0.5$. In terms of the probability function $\eta(p)$, we can calculate the mean value $\bar{p}$ and the relative standard deviation δ as

$$\bar{p} = \sum_{p} p\eta(p) = 0.49747 \tag{29}$$

and

$$\delta = \frac{1}{\bar{p}}\left(\sum_{p}(p-\bar{p})^2\eta(p)\right)^{1/2} = 0.18692 , \tag{30}$$

respectively.

The simulation shows that the jumps from GS to EIC occur in a rather broad region, which is the transitional region (Fig. 2). For the probability distribution $\eta(p)$, its peak position p_M and the mean value $\bar{p}$ are close to p_c defined in Eq. (23). This may indicate that

Table 4
Probability distribution functions Ψ_n and η_n, slow jump case, $N = 10$ and $L_c = 1.0$

n	0	1	2	3	4	5	6	7	8	9	10
ν_n	-	10	90	280	406	292	100	28	0	0	0
μ_n	-	0	0	14	125	185	86	28	0	0	0
Ψ_n	-	0	0	0.05	0.3079	0.6560	0.86	1	-	-	-
η_n	-	0	0	0.0320	0.2853	0.4224	0.1964	0.0639	0	0	0

the conversion to EIC mode could be attributed to a percolation transition of the equivalent damage region merely in the sense of averaging or highest probability because it has quite a large relative width δ. So, EIC is inherently different from the usual percolation.

Fast jump (Case 3). In this case, the rate of stochastic jump is higher than that of pattern dynamics, hence the jumps from all states, both transient and fixed states, are important. The number of possible jumps from the states in group $(n-1)$ to the states in group n is given by

$$\nu_n = (N - n + 1)\Omega_{n-1} = n\Omega_n , \tag{31}$$

which includes all jumps of GS to GS, GS to EIC and EIC to EIC (Fig. 3b). It is easy to deduce that the number of jumps from GS states in group $(n-1)$ to EIC states in group n is

$$\mu_n = (\Phi_n - \Phi_{n-1})\nu_n \tag{32}$$

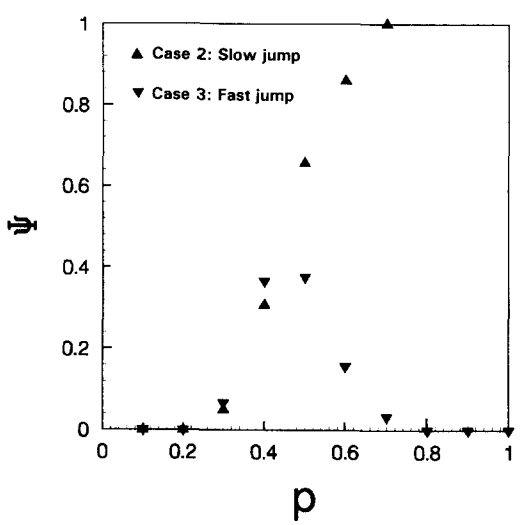

Fig. 4. Effect of rate on failure probability ($N = 10$, $L_c = 1.0$). ▲: Case 2, Slow jump; ▼: Case 3, Fast jump.

From Eqs. (25), (26) and (32), it is found that

$$\Psi_n = \Phi_n - \Phi_{n-1} . \tag{33}$$

and

$$\eta_n = \frac{\nu_n}{\mu}(\Phi_n - \Phi_{n-1}) \tag{34}$$

From Eqs. (33) and (34), we can see that the nonzero region of $\Psi(p)$ and $\eta(p)$ is also $p_L < p \leq p_U$, which is again the transitional region. As an example, the results of the chain of $N = 10$ and $L_c = 1.0$ are shown in Table 5. In the fast jump case, both $\Psi(p)$ and $\eta(p)$ are unimodal functions (see Fig. 4). The peak is at $p_M = 0.5$, the mean value is $\overline{p} = 0.49012$ and the relative standard deviation is $\delta = 0.16851$. Once more, $\tilde{p} \sim p_M = p_c$. Simulations of different chains, i.e. various values of N and L_c, for both fast and slow jump cases show similar characteristics in the probability distribution functions $\Psi(p)$ and $\eta(p)$.

4. Conclusion

In order to obtain some insight in the effect of various rate processes on the interplay of disorder and failure, an abstract and simple evolution chain model is investigated in this paper. The model includes some effects of two important processes observed experimentally in failure phenomena, i.e. nucleation and coalescence of damages. These are modeled by the coupling effect of stochastic jump and dynamical evolution. The latter is governed by a nonlinear and nonlocal dynamical rule, namely the load sharing rule in mechanics. The damage evolution can be divided into globally stable (GS) and evolution induced catastrophic (EIC) mode, the latter corresponds to macroscopic failure of materials. The conversion from GS to EIC can be induced by a stochastic jump of pattern. The coupling

Table 5
Probability distribution functions Ψ_n and η_n, fast jump case, $N = 10$ and $L_c = 1.0$

n	0	1	2	3	4	5	6	7	8	9	10
ν_n	–	10	90	360	840	1260	1260	840	360	90	10
μ_n	–	0	0	24	308	474	198	28	0	0	0
Ψ_n	–	0	0	0.0667	0.3667	0.3762	0.1571	0.0333	0	0	0
η_n	–	0	0	0.0233	0.2985	0.4593	0.1919	0.0271	0	0	0

between these two rate processes strongly affects the failure probability.

It is found that the transitional region, where the GS and EIC modes coexist, plays an important role in the damage evolution. It implies that the damage evolution cannot be determined by a damage fraction uniquely, but is sensitively dependent on the initial configuration of damage. That is to say, the system shows a distinctive pattern-specific behavior. Then, the appearance of EIC should be characterized by probability distribution functions $\Phi(p), \xi(p), \Psi(p)$ and $\eta(p)$, rather than a definite threshold of damage fraction. The characteristics of these failure probability functions are distinctively different owing to the rate effect. Although the obtained results are based on an abstract and quite simple model, they may provide a framework for a deeper understanding of failure phenomena in real materials.

Acknowledgements

This work is jointly supported by the National Fundamental Research Project "Nonlinear Science", the National Natural Science Foundation of China and the Chinese Academy of Sciences under Special Grant "KM85-33". We are indebted to Prof. P. Li for her careful reading of the manuscript and valuable advices in the revision.

References

[1] See, for example, D.R. Curran, L. Seaman and D.A. Shockey, Dynamic failure of solids, *Phys. Rep.* 147, 253–388 (1987).
[2] H.J. Herrmann and S. Roux (eds.), *Statistical models for the fracture of disordered media* (Elsevier, Amsterdam, 1990).
[3] B.B. Mandelbrot, D.E. Pasoja and A.J. Paullay, Fractal character of fracture surface, *Nature* 308, 721–722 (1984).
[4] O. Pla, F. Guinea, E. Louis, G. Li, L.M. Sander, H. Yan and P. Meakin, Crossover between different growth regime in crack formation, *Phys. Rev.* A 42, 3670–3673 (1990).
[5] P. Meakin, Models for material failure and deformation, *Science* 252, 226–234 (1991).
[6] L. de Arcangelis, Scaling behaviour in fracture models, *Physica Scripta* T 29, 234–238 (1989).
[7] H.J. Herrmann, Patterns and scaling in fracture, *Physica Scripta* T 38, 13–21 (1991).
[8] E. Louis and F. Guinea, Fracture as a growth process, *Physica* D 38, 235–241 (1989).
[9] H.J. Herrmann, Fractal deterministic cracks, *Physica* D 38, 192–197 (1989).
[10] M. Sahimi and S. Arbabi, Percolation and fracture in disordered solids and granular media: approach to a fixed point, *Phys. Rev. Lett.* 68, 608–611 (1992).
[11] T.L. Chelidze, Percolation and fracture, *Phys. Earth Planet. Int.* 28, 93–101 (1982);
Percolation theory as a tool for imitation of fracture process in rocks, *Pure Appl. Geophys.* 124, 731–748 (1986).
[12] P. Bak, C. Tang and K. Wiesenfield, Self-organized criticality, *Phys. Rev.* A 38, 364–374 (1988).
[13] P.M. Duxbury and P.L. Leath, Failure probability and average strength of disordered systems, *Phys. Rev. Lett.* 72, 2805–2808 (1994).
[14] Y. Bai, Z. Ling, L. Luo and F. Ke, Initial development of microdamage under impact loading, *Trans. ASME, J. Appl. Mech.* 59, 622–627 (1992).
[15] Y. Bai, M. Xia, F. Ke, C. Lu and Z. Ling, Analysis and simulation of evolution induced catastrophe, *Chinese, Phys. Lett.* 10, 155–158 (1993).
[16] Y. Bai, C.S. Lu and W.S. Han, Statistical evolution of microcracks and evolution induced catastrophe in spallation, *Proc. IUTAM Int. Symp. on Impact Dynamics*, ed. Zheng Zhemin (Peking Univ. Press, 1994) 234–241.
[17] Y. Bai, C. Lu, F. Ke and M. Xia, Evolution induced catastrophe, Phys. Lett. A 185, 196–200 (1994).
[18] M. Xia, Y. Bai and F. Ke, Statistical description of pattern evolution in damage-fracture, *Science in China* A 37, 331–340 (1994).
[19] R.E. Pitt and S.L. Phoenix, Probability distribution for the strength of composite material. III. The effect of fiber arrangement, *Int. J. Fract.* 20, 291–311 (1982).
[20] S.L. Phoenix et al., Statistics for the strength and lifetime in creep-rupture of model carbon/epoxy composites, *Comp. Sci. Tech.* 32, 81–120 (1988).